CHAPTER 6: Development of TRPA1 siRNA Based Nanoformulation for the Treatment of Chemotherapy-Induced Neuropathic Pain

6.1 Introduction

Despite several efforts by scientists in the last decades, to date, there are no effective treatments available so far for Chemotherapy-induced neuropathic pain (Sánchez et al., 2023). Most of the clinically available therapeutics for neuropathic pain did not work in the case of CINP patients as the cellular and molecular etiology associated with both pathologies is distinct. Chemotherapy leads to the development of peripheral neuropathy by striking the somatosensory nervous system, increasing the neuronal firings and activation of nociceptive mediators including transient receptor protein ankyrin 1 (TRPA1). TRPA1 belongs to the TRP superfamily, and it is a nonselective Ca^{2+} cation channel that gets activated by capsaicin, heat and other endogenous and exogenous ligands. TRPA1 is widely distributed on nociceptive neurons of the peripheral system and studies have suggested that the higher expression of TRPA1 in dorsal root ganglions (DRG) plays a vital role in the development of CINP (Staruschenko et al., 2010; Zaki et al., 2022). Pharmacological or genetic inhibition of TRPA1 has been shown to diminish the responses of nociceptive primary afferent nerve fibers to noxious mechanical stimulation. The limb withdrawal response to mechanical stimulation was notably reduced when TRPA1 was specifically deleted in sensory neurons. Several reports suggest that CINP significantly upregulates the TRPA1 expression in rats (Staaf et al., 2009). In our previous studies, we have investigated the effect of chemotherapy on the modulation of pain-regulatory genes in rats, we demonstrated that chemotherapy treatment significantly up-regulated TRPA1 mRNA

and protein expressions in the DRG and spinal cord of neuropathic rats. Notably, despite this upregulation, it is widely reported that TRPA1 antagonists are commonly employed to alleviate various pain modalities, including CINP, exhibits severe side effects such as respiratory depression, allergic reactions, and cardiovascular deformities. Consequently, there is a critical need for a specific tool to silence or knockdown the TRPA1 gene, providing a more targeted intervention and minimizing the risk of off-target effects associated with antagonists. Recently, RNA interference (RNAi) has emerged as a powerful tool for gene silencing by neutralizing targeted mRNA molecules, gaining popularity in the realm of targeted interference for pain regulation. The FDA's approval of RNAi-based therapeutics in 2018 marked a pivotal moment, steering research and market values towards the potential of RNAi-based gene therapy in clinical applications. Notably, TRPV1-based RNAi therapy is progressing through clinical trials for ocular pain (phase I) and dry eye syndrome (phase II). This underscores the promising potential of TRPA1 siRNA-based gene therapy as a modality for both the prevention and management of CINP.

Utilizing small interfering RNA (siRNA) as a potent tool for treating diseases involves inhibiting the expression of targeted proteins linked to disease progression. However, two key challenges impede siRNA therapeutics implementation. Firstly, siRNA faces instability in the bloodstream, undergoing rapid degradation by nucleases. Additionally, siRNA encounters difficulty traversing cell membranes without complexation with unsuitable in vivo transfection reagents. Overcoming these hurdles, lipid nanoparticle (LNP) delivery systems prove effective for siRNA delivery. These lipid nanoparticles (LNPs) protect the siRNA cargo, prevent degradation, and facilitate cellular uptake while avoiding renal clearance. An illustrative example of nanoparticle

application is seen in the clinical translation of mRNA vaccines against COVID-19 by Moderna and Pfizer/BioNTech, receiving FDA emergency use authorization in 2020. Given the collective evidence, RNAi-based therapies present an opportunity for customization to suit individual patient and this approach allows for a personalized strategy in addressing CINP. Liposomes have been used successfully to deliver conventional drugs or new genetic drugs including plasmid DNA-containing therapeutic genes, antisense oligonucleotides (ASO), and small interfering RNA (siRNA) in preclinical models and clinical trials (Fernando et al., 2018).

6.2 Experimental design

Initially, in-vivo validation and knockdown efficacy of TRPA1 siRNA were assessed in healthy rats through intrathecal administration. Efficacy and specificity were confirmed by administering TRPA1 siRNA via intrathecal injection (lumbar L4-L6 vertebrae). RT-PCR and western blot analyses were conducted to measure TRPA1 mRNA and protein expression levels in healthy rats. Following successful in vivo validation, blank and encapsulated TRPA1 siRNA liposomal formulations were prepared using DOTAP/chol liposomal via the thin-film evaporation method. DOTAP/CHOL at molar ratios of 1:1, 1:2, and 1:3 was dissolved in chloroform, and the solvent was evaporated to generate a thin lipid film. Hydration with phosphate-buffered saline resulted in a homogeneous liposomal solution, which was then extruded through 200-nm and 100-nm polycarbonate membranes. Cationic liposomes were complexed with anionic siRNA, and the hydrodynamic diameter, polydispersity index (PDI), and zeta potential were determined by dynamic light scattering (DLS). Morphological characterization was performed using scanning electron microscopy, high resolution transmission electron microscopy and atomic force microscopy. The characterization extended to infrared

spectroscopy (ATR method), X-ray photoelectron spectroscopy, thermogravimetric analysis, and differential scanning calorimetry to gain insights into the structural and thermal characteristics, stability, and elemental composition of the formulated particles under specific conditions. We assessed baseline pain levels in rats prior to chemotherapy administration (day 0). Post-chemotherapy, on day 14 (designated as day 1, when pain was at its peak), we administered TRPA1 siRNA formulations and various controls via intrathecal (lumbar puncture) and intravenous routes from day 1 to day 6. Daily evaluations of therapeutic efficacy were conducted using behavioral assays for mechanical allodynia and cold allodynia, given the TRPA1 gene's role in neuropathic pain. Upon the diminishment of the formulations' effects, the animals were euthanized, and dorsal root ganglia (DRG) and spinal cord tissues were collected for further cellular and molecular analyses to elucidate the mechanisms underlying the formulation's efficacy in mitigating CINP. No harmful effects of TRPA1 siRNA were observed, as confirmed by neurobehavioral assays including rota rod and open field tests. This comprehensive approach allowed us to thoroughly investigate the therapeutic potential and safety of TRPA1 siRNA formulations in the context of CINP.

6.3 Results and discussion

6.3.1 Validation of TRPA1-siRNA knockdown efficacy in rats

The spinal circuits and interneurons located within the dorsal horn of the spinal cord play a crucial role in the transmission and processing of sensory information, including both pain and touch sensations. This function becomes particularly significant during instances of CINP. In our study, we aimed to investigate the potential impact of silencing the TRPA1 gene using siRNA in naïve rats. Before generating liposomal encapsulated TRPA1 siRNA nanoparticles, we confirmed the efficacy and specificity

of siRNA. We administered TRPA1 siRNA through intrathecal Injection (lumber L4-L6 vertebra) to assess the effectiveness of gene knockdown and performed real-time polymerase chain reaction (RT-PCR) to measure the expression levels of TRPA1 mRNA. Our findings suggest significant reduction in TRPA1 mRNA expression in the spinal cord of rats that received the TRPA1 siRNA as compared to scrambled siRNA treated group **(Figure 6.1)**. Furthermore, we sought to validate the efficacy of TRPA1 gene silencing using western blotting analysis. Our results consistently demonstrate a significant decrease in TRPA1 protein expression TRPA1 siRNA administered rats, as compared to scrambled siRNA treated group **(Figure 6.2)**. Recognizing the pivotal role of nociceptive DRG neurons in the development of CINP, we specifically examined the effect of TRPA1 gene silencing in these neurons. Intriguingly, our investigations did not reveal any significant alterations in either TRPA1 mRNA or protein expression within the DRG neurons, as compared to the scramble siRNA. In summary, this study provides compelling evidence for the successful downregulation of TRPA1 gene expression within the spinal cord following lumber injection of TRPA1 siRNA. This downregulation was confirmed through both molecular techniques RT-PCR and western blotting. However, it's noteworthy that the effect of TRPA1 gene silencing in DRG neurons was not as evident, suggesting potential complexities in the gene regulation within these specific neurons during this intervention.

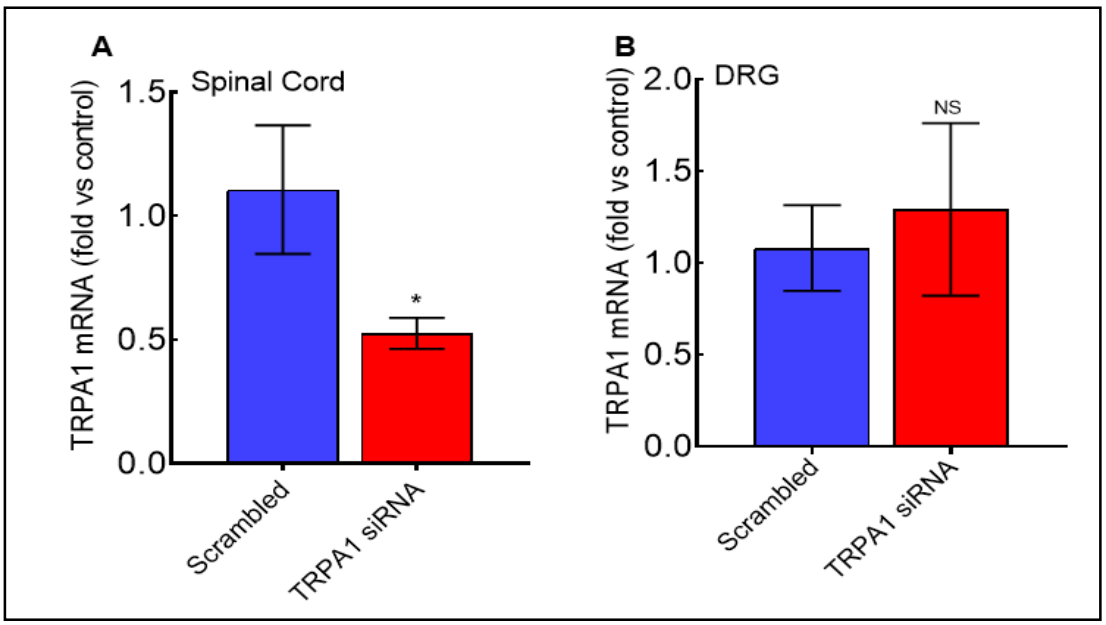

Figure 6.1 Effect of siRNA in TRPA1 mRNA expression in rats A) mRNA expression in spinal cord. B) mRNA expression in DRG. Data were reported as mean ± SEM. ***P<0.001 indicates statistical significance as compared to the naïve rats. P<0.05 was considered statistically significant.

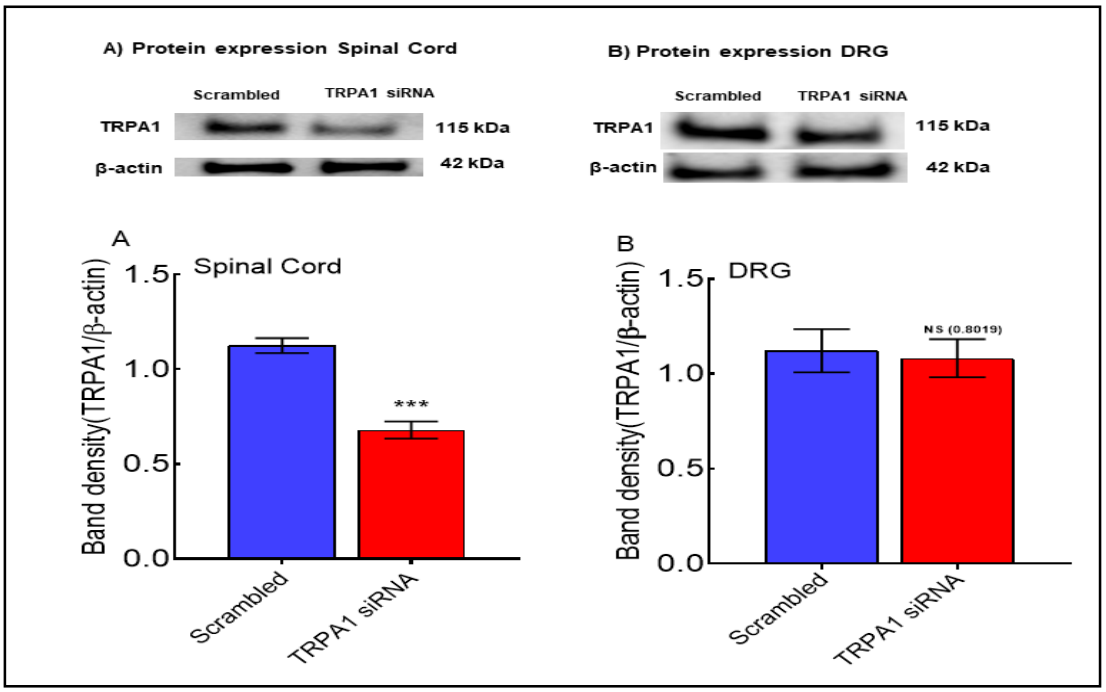

Figure 6.2. Effect of siRNA in TRPA1 protein expression in rats A) Protein expression in spinal cord. B) Protein expression in DRG. Data were reported as mean ± SEM. ***P<0.001 indicates statistical significance as compared to the naïve rats. P<0.05 was considered statistically significant.

6.3.2 Physicochemical Characterization of blank liposome and TRPA1 siRNA loaded liposome

The results of particle size, zeta potential, and PDI analysis are presented in Table 1. PDI analysis was carried out to measure the width of unimodal size distributions. A PDI value below 0.7 is considered acceptable for a monodisperse and polydispersity particle size distribution, the PDI value should be < 0.5 and > 1, respectively (Mokhtarieh et al., 2018; Sun et al., 2022). We have performed the particle size, PDI, and ζ-potential between blank liposome and siRNA loaded liposome following the complexation with siRNA, the mean particle size (both $p < 0.0001$) an PDI ($p < 0.0001$) increased, while the ζ-potential ($p < 0.0001$) of the siRNA was decreased. This indicated that adding a negatively charged large molecule such as siRNA to the lipid-based particles might induce large, less uniformly distributed complexes compared to blank liposome. A small PDI value indicated good dispersion homogeneity of the nanoparticles. TRPA1 siRNA loading lead to little bit increase in the size of siRNA loaded liposome (198.9±1.6 nm) as compared to the blank liposome (189.3 ±2.5 nm). The particle aggregation can be determined by comparing the data obtained from differential scanning calorimetry (DLS) and transmission electron microscope (TEM) studies. Interestingly, we did not observe any significant difference in particle size of siRNA loaded as compared to the blank liposome. the published reports also suggested the size of aggregated suspension in HR-SEM and DLS analysis (Gupta et al., 2014). HR-TEM micrographs of prepared liposome were shown in **Figure 6.3**. and it has also verified the size of prepared liposomes was in the acceptable ranges from 180−200 nm also confirmed the spherical shape of vesicles (**Figure 6.4**). The presence of diffused rings in selected area electron diffraction pattern (SAED) images is indicative of the crystalline and amorphous nature of material. We

have found that the diffused rings were not find in SAED images, indicating the amorphous nature of the prepared liposomes (Figure 6.4).

Table 6.1: Particle size, zeta potential and poly dispersity of blank and siRNA loaded liposomes. Data are expressed as mean ± SEM of three separate experiments for both samples (Blank Liposomes, and siRNA loaded liposomes), with five measurements for each. The true PDI is Z average only.

Sample code	Particle size (nm)	Zeta potential (mV)	Poly dispersity index (PDI)
Blank Liposomes	189.3 ±2.5	31.6±1.1	0.283 ± 0.02
siRNA loaded Liposomes	198.9±1.6	26.1±1.3	0.302±0.05

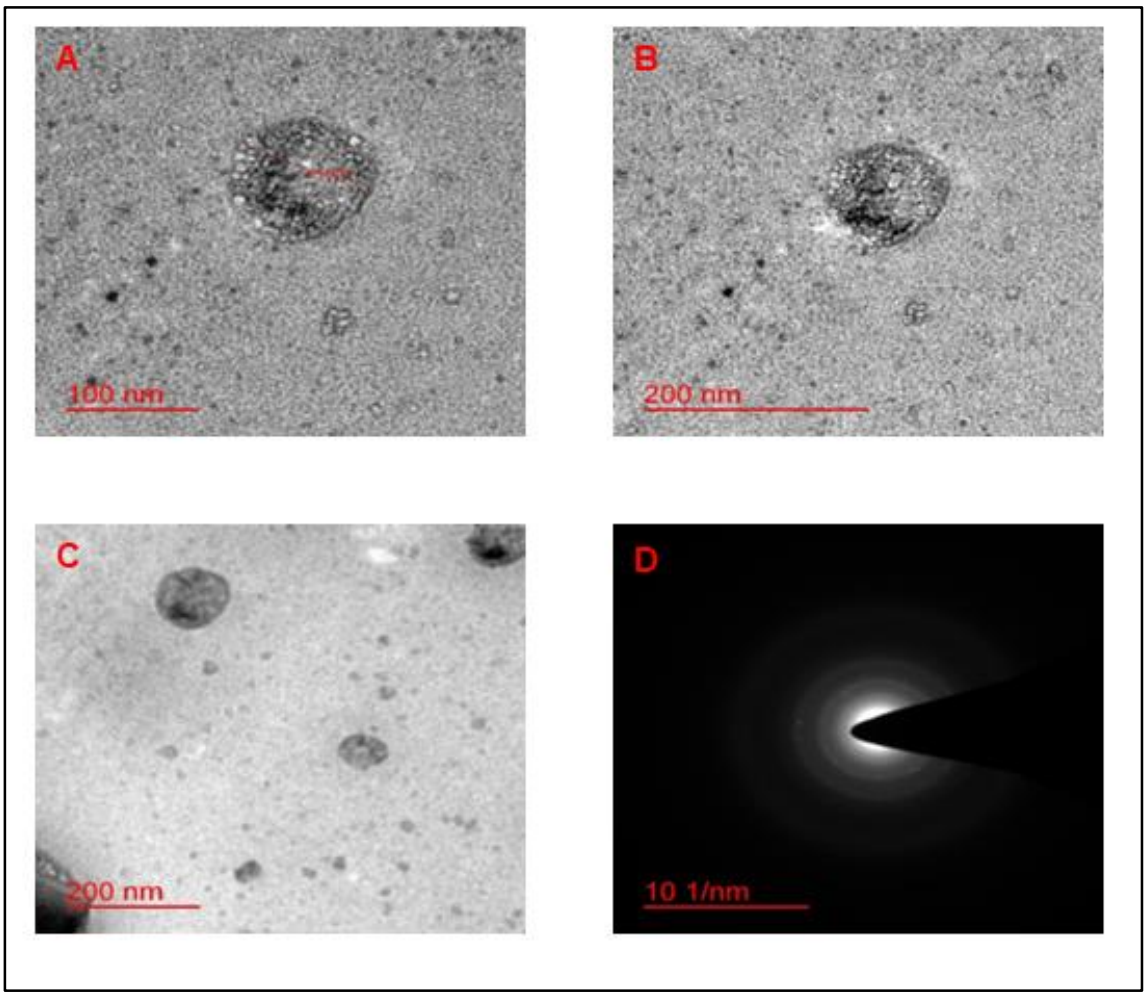

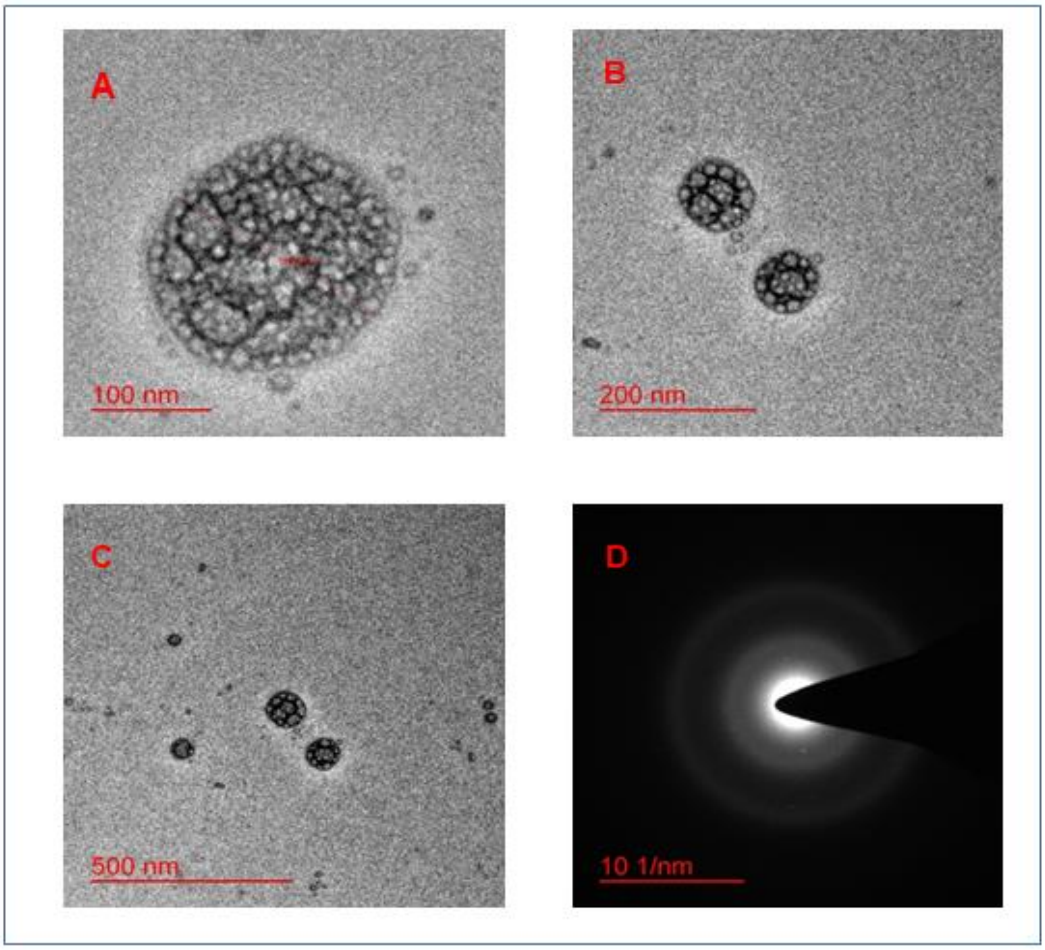

Figure 6.3 A) High resolution transmission electron microscopy (HR-TEM) of blank-liposome **(A)** at 100 nm, **(B)** at 200 nm **(C)** at 500 nm**. D)** Selected area electron diffraction pattern (SAED) micrograph of blank liposome. **B)** (HR-TEM) of siRNA loaded-liposome **(A)** at 100 nm, **(B)** at 200 nm **(C)** at 500 nm**. D)** Selected area electron diffraction pattern (SAED) micrograph of blank liposome.

6.3.3 Scanning electron microscopy (SEM) Analysis

SEM images provide conclusive evidence regarding the successful fabrication of homogenous and distinctly isolated liposomal carriers encapsulating siRNA molecules, as depicted in the accompanying figure. SEM micrographs showcasing the morphology of the liposomes are illustrated in the figure for both formulations.

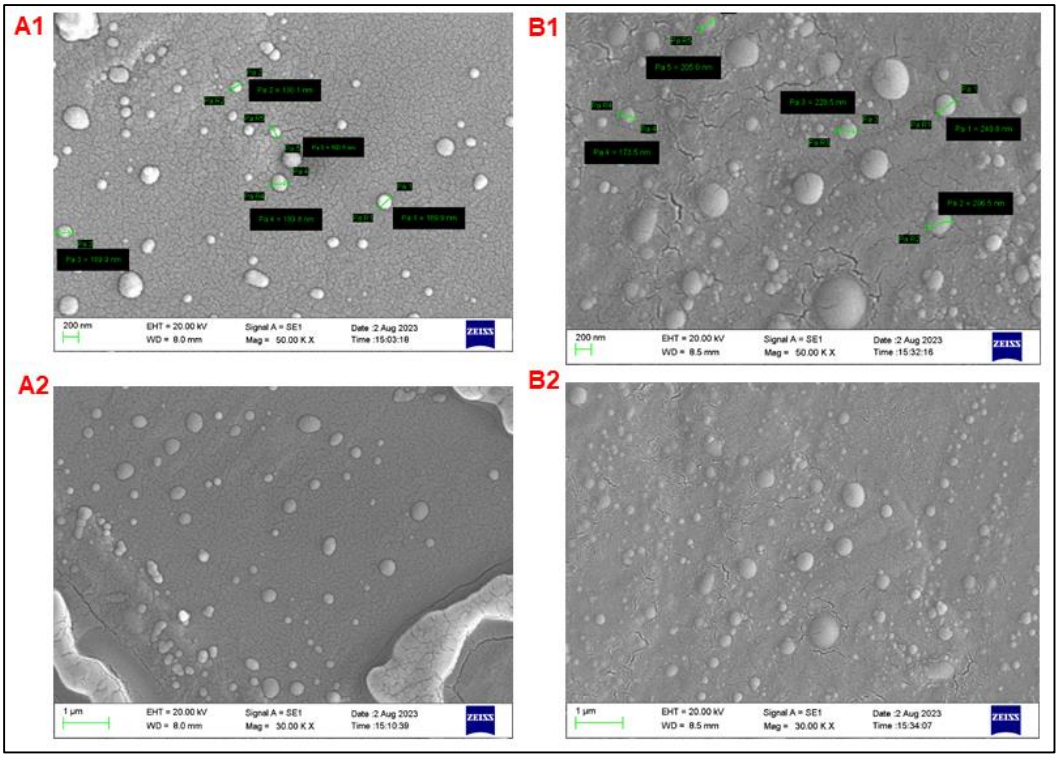

Figure 6.4 Representative images of liposome formulations. (a) SEM images at 2.00 kV with a scale bar of 200 nm: a. The morphology of lipo-siRNA showing a smooth sphere in the size range of ≥200 nm; b. The morphology of bare liposome showing a coarse sphere in the size range of ≤200 nm.

Further confirmation was also done with the help of high resolution scanning electron microscopy (HR-SEM) analysis. It showcases the morphology of the liposomes are illustrated in the figure for both blank and liposomal formulations of TRPA1 siRNA.

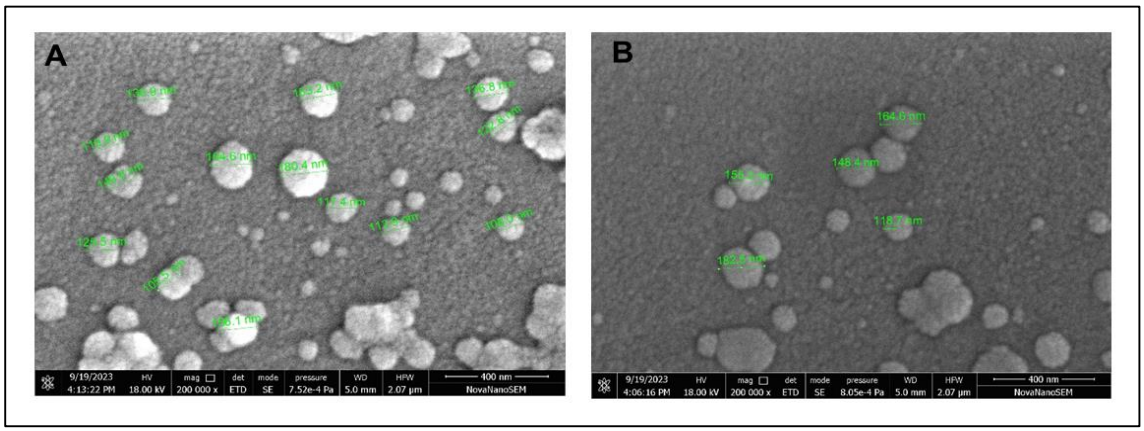

Figure 6.5 Representative images of blank and liposome formulations. HR-SEM images at 2.00 kV with a scale bar of 400 nm: A) The morphology of blank formulation

showing a smooth sphere in the size range of ≥170 nm; B) The morphology of TRPA1 liposome showing a coarse sphere in the size range of ≤200 nm.

6.3.4 Atomic Force Microscopy (AFM) analysis

Our prepared formulation has unveiled intricate structural intricacies at the nanoscale level. The AFM images have provided three-dimensional (3D) renderings of the samples, elucidating surface characteristics within the nanometer range, as depicted in the accompanying figure. Notably, the homogenous TRPA1 siRNA-loaded liposomal formulation exhibited root-mean-square (Ra) and roughness average (Rq) values measuring 19.179 nm and 14.590 nm, respectively. The AFM images further revealed spherical-shaped blank liposomes, characterized by a root-mean-square (Ra) value of 2.463 nm and a roughness average (Rq) of 1.295 nm (**Figure 6.6)**. This observation underscores the high homogeneity and smooth surface of the blank liposomes, as portrayed in the figure. Significantly, it is evident that the introduction of siRNA loading into the liposomal structure prompted a notable increase in surface roughness, resulting in a Ra value of 19.179 nm. This augmentation in surface roughness within the siRNA-loaded liposomal structure is attributed to the presence of distinct elevations on the surface, corresponding to the encapsulated siRNA molecules. This insight underscores the effect of siRNA encapsulation on altering the topographical attributes of the liposomal surface.

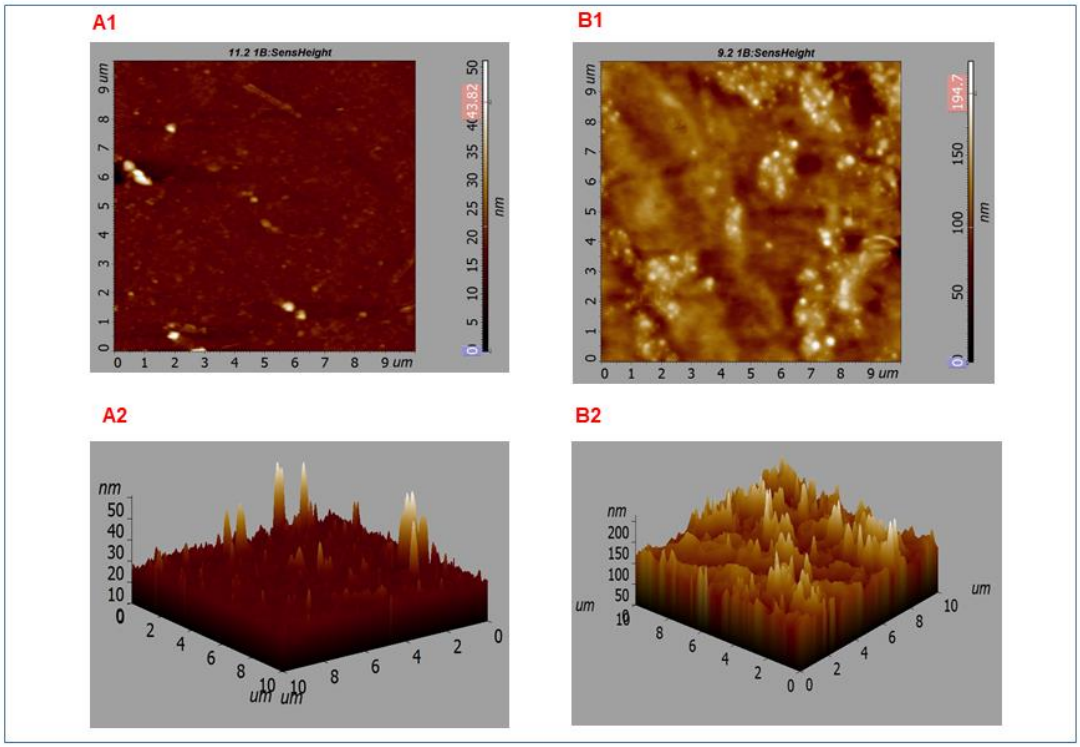

Figure 6.6 Atomic force microscopy (AFM) images of TRPA1 siRNA-loaded liposomal formulation: AFM studies were carried out for the three-dimensional morphological characterization of blank and siRNA-loaded liposomes. **A1)** 2D images **A2)** 3D image (Root mean square (Ra) and Roughness average (Rq) were 2.463 nm and 1.295 nm, respectively). **B1)** 2D images **B2)** 3D image (Root mean square (Ra) and roughness average (Rq) were 19.179 nm and 14.590 nm, respectively).

6.3.5 Fourier-transform infrared analysis of liposome

The Fourier-transform infrared (FTIR) spectra of the TRPA1 siRNA-loaded liposomal formulation have been examined. The spectrum originating from the blank liposome (comprising DOTAP and cholesterol components) displayed discernible peaks at 1740 cm^{-1}, attributed to the stretching of carbonyl bonds. Additionally, faint bands corresponding to various bending modes of C-H bonds appeared below 1450 cm^{-1}. The presence of a peak at 1468 cm^{-1} can be linked to the -CN stretching from the amino headgroups within the DOTAP molecule. However, a significant band at 1105 cm^{-1} emerged in the DOTAP spectrum, signifying the antisymmetric stretching

vibrations of C(O)=OR in the lipid ester group. The distinctive characteristic peak of the DOTAP-Cholesterol liposome formulation was evident at 2925 cm^{-1}. The most pronounced features include absorption bands influenced by the symmetric and asymmetric stretching vibrations of C-H bonds within the CH_2 groups of DOTAP's acyl chains. Additionally, a broad peak at 3400 cm^{-1}, attributable to the presence of OH groups in cholesterol, was observed (as depicted in the **Figure 6.7**). Crucially, the repeated appearance of all these peaks in the subsequent figure underscores the absence of any chemical interaction between siRNA and the constituents, namely DOTAP and cholesterol, within the liposomal formulation **Figure 6.7**. This observation supports the conclusion that the encapsulation process does not induce significant chemical alterations in the interactions between siRNA and the liposomal components.

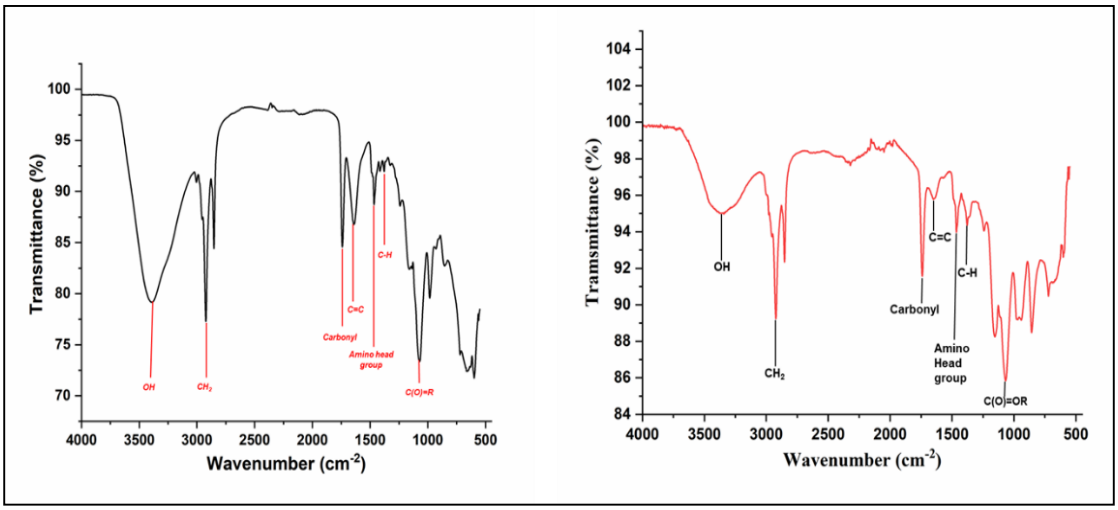

Figure 6.7 FTIR spectra of TRPA1 siRNA-loaded liposomal formulation: A) Absorption bands near 3500 cm^{-1}, 3000 cm^{-1}, and 1500 cm-1 in the FTIR spectrum of blank liposome reflected bending, symmetric stretching, and asymmetric stretching, respectively. B) Absorption bands near 3500 cm^{-1}, 3000 cm^{-1}, and 1500 cm-1 in the FTIR spectrum of siRNA loaded liposome reflected bending, symmetric stretching, and asymmetric stretching, respectively.

6.3.6 Differential Scanning Calorimetry (DSC) analysis

DSC of the TRPA1 siRNA-loaded liposomal formulation provides valuable insights into the thermal stability and interactions within the complex system. The results exhibit distinct thermal behavior: The DSC thermogram of DOTAP, a constituent of the liposome, manifests endothermic peaks at 50.9 °C and 152.5 °C. Conversely, the Lipo-blank composition, comprising cholesterol and DOTAP, showcases endothermic peaks at 46.2 °C, 85.88 °C, 117.13 °C, and 192.6 °C. The formation of liposomes induces shifts in these endothermic peaks. However, the thermogram of the siRNA-loaded liposome experiences notable endothermic peak shifts, observed at 89.2 °C and 203.5 °C. These peaks exhibit a relatively wider profile compared to the blank liposomes **Figure 6.8**. Remarkably, these endothermic peaks correspond to the characteristic peaks of its constituents, such as cholesterol and DOTAP. The broadening and vanishing of endothermic peaks in the thermogram signify alterations in the regularity of the lipid structure. In simpler terms, the introduction of DOTAP serves to reduce the membrane's rigidity, consequently promoting a more fluidic nature. This thermal analysis thereby underscores the dynamic changes in the liposomal structure resulting from the incorporation of siRNA and DOTAP, potentially influencing their functional properties.

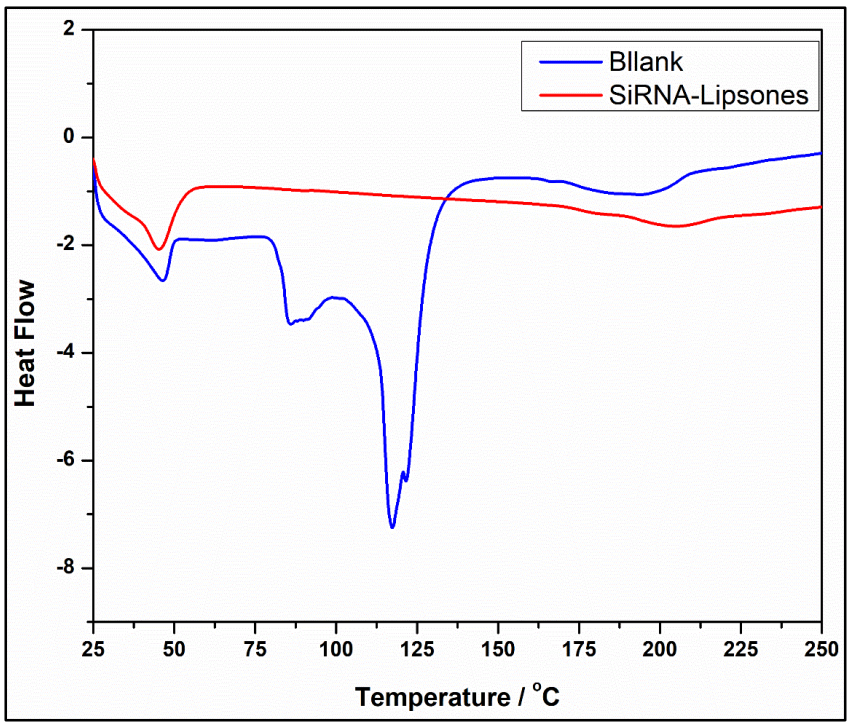

Figure 6.8 Differential scanning calorimetry curves of TRPA1 siRNA-loaded liposomal formulation: A) The Differential scanning calorimetry (DSC) of blank liposomes is presented. It shows that Flat curves without any endothermic peak confirmed the stability of the liposome carriers. B) DSC of siRNA loaded liposome.

6.3.7 Thermogravimetric Analysis (TGA) of liposome formulation

TGA serves as a crucial tool in the characterization of blank liposomes and siRNA-loaded liposomal formulations, offering a comprehensive understanding of their thermal properties. TGA involves subjecting samples to controlled temperature ramps while monitoring their weight changes. In the case of blank liposomes, TGA can reveal the thermal stability and degradation temperatures of the lipid bilayer, as well as any potential water content within the formulation. Additionally, for the siRNA-loaded liposomal formulation, TGA enables the assessment of the interaction between siRNA and lipids, and provides insights into the stability of siRNA within the liposomes. Weight loss observed in the TGA curve may indicate the removal of water, lipid melting, or degradation of the encapsulated siRNA. By comparing the TGA curves of

blank liposomes and siRNA-loaded liposomes, researchers can discern the impact of siRNA encapsulation on the overall thermal behaviour and stability of the liposomal formulation **Figure 6.9**. This information is vital for evaluating the suitability of the formulation for biomedical applications, where thermal stability plays a pivotal role in ensuring the integrity and effectiveness of the delivered cargo. To assess the stability of both the blank liposome and the siRNA loaded liposome, a thorough examination was conducted using thermogravimetric analysis (TGA) spectroscopy. This analysis involved studying lyophilized liposome samples. The TGA experiments were carried out under a nitrogen atmosphere.

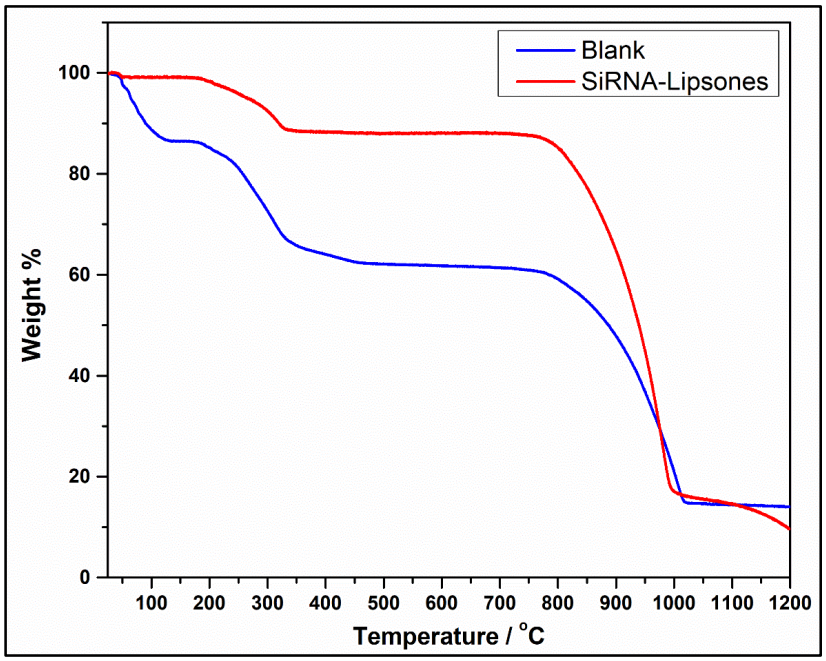

Figure 6.9. Thermogravimetric analysis (TGA) of blank and siRNA loaded liposome A) TGA weight loss results under a nitrogen environment show that the blank liposome. **B)** weight loss of TRPA1 siRNA loaded liposomal formulation.

6.3.8 X-ray photoelectron spectroscopy (XPS) analysis

XPS analysis of the siRNA-loaded liposomal formulation provides crucial insights into the elemental composition and surface chemistry of the material. By

utilizing X-ray irradiation to elicit photoelectrons from the material's surface, the resulting kinetic energy and number of emitted electrons enable the identification of present elements and their chemical states. XPS analysis was carried out to confirm the loading of siRNA in liposomes and to detect the presence of desired elements in blank liposome and siRNA loaded liposome. O 1s and N 1s spectra contained a single peak centred at 532.5 eV and 402.0 eV, respectively, indicating presence of hydroxyl group and quaternary ammonium head group. Cl 2p spectra had a two-peak centred at 198.0 eV and 196.0 eV, indicating presence of chlorine atoms. Signals of O, C, N, Cl, S, and P were detected in the survey spectrum of siRNA loaded liposome, indicating successful loading of siRNA in liposome. XPS survey spectra for blank liposome and siRNA loaded liposome are shown in Figure. Individual characteristic peaks are shown in figure. XPS spectrum of the siRNA-loaded liposomal formulation offers valuable insights into the elemental composition and chemical environment of the material's surface. XPS utilizes X-ray irradiation to eject photoelectrons from the sample's surface, and the kinetic energy and number of these emitted electrons are used to identify the elements present as well as their chemical states. In the context of the siRNA-loaded liposomal formulation, the survey spectrum can provide information about the distribution of elements such as carbon, oxygen, nitrogen, and potentially other trace elements **(Figure 6.10)**. By comparing the survey spectrum of the siRNA-loaded formulation to that of blank liposomes, researchers can assess any chemical changes resulting from siRNA incorporation or interactions between the encapsulated siRNA and the lipid matrix. This analysis can reveal alterations in the chemical bonding and oxidation states, shedding light on the surface chemistry of the formulation. Understanding these surface-level changes is crucial for evaluating the stability and

compatibility of the siRNA-loaded liposomal formulation for its intended biomedical applications.

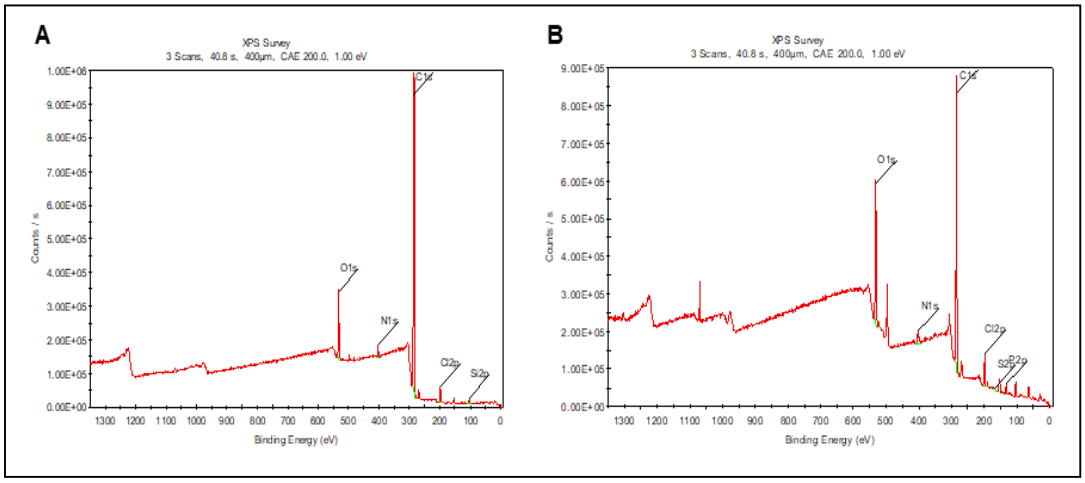

Figure 6.10 X-ray photoelectron spectroscopy (XPS) survey spectrum of siRNA-loaded liposomal formulation: A) X-ray photoelectron spectroscopy (XPS) analysis was carried out to confirm the successful synthesis of blank liposome and to detect the presence of desired elements. **B)** siRNA loaded liposome and to detect the presence of desired elements.

In summary, the characterization outcomes indicate the successful development and validation of a liposomal formulation containing TRPA1 siRNA.

6.4 Agarose gel electrophoresis for entrapment efficiency of TRPA1 siRNA liposome

The gel electrophoresis results reveal the entrapment efficiency of TRPA1 siRNA in the liposomal formulation (Cun et al., 2011; Katas and Alpar, 2006; Park et al., 2013). The migration pattern in each lane provides insights into the presence and integrity of TRPA1 siRNA within the liposomes. The DNA ladder marker in Lane 1 serves as a reference for estimating the size of the siRNA fragments. Interpretation of the gel electrophoresis bands will provide valuable information regarding the success of TRPA1 siRNA encapsulation in the liposomes. The comparison between Lane 2 (TRPA1 naked siRNA) and Lane 3 (TRPA1 siRNA liposome) allows for the assessment of siRNA protection and encapsulation efficiency achieved through the

liposomal formulation. Lane 1 (DNA ladder marker): The DNA ladder marker serves as a reference for estimating the size of the TRPA1 siRNA fragments. It typically consists of a mixture of DNA fragments of known sizes, forming a ladder-like pattern when separated on the gel. The bands in this lane allow for the determination of the size range of the siRNA fragments. Lane 2 (TRPA1 naked siRNA): The bands in this lane represent the migration pattern of TRPA1 siRNA without any protective or encapsulating structure. The presence and intensity of bands in this lane indicate the integrity and size distribution of the naked siRNA. Comparing this lane with the ladder marker helps confirm the expected size range of TRPA1 siRNA. Lane 3 (TRPA1 siRNA Liposome): The bands in this lane reveal the migration pattern of TRPA1 siRNA that has been encapsulated within the liposomal formulation. The goal is to observe whether the siRNA remains protected and contained within the liposomes and the presence and intensity of bands in this lane, in comparison to Lane 2 and the ladder marker, provide insights into the success of siRNA encapsulation (**Figure 6.11)**. Subsequently, we evaluated the therapeutic effectiveness of this developed nanoscale formulation in an animal model of chemotherapy-induced neuropathic pain.

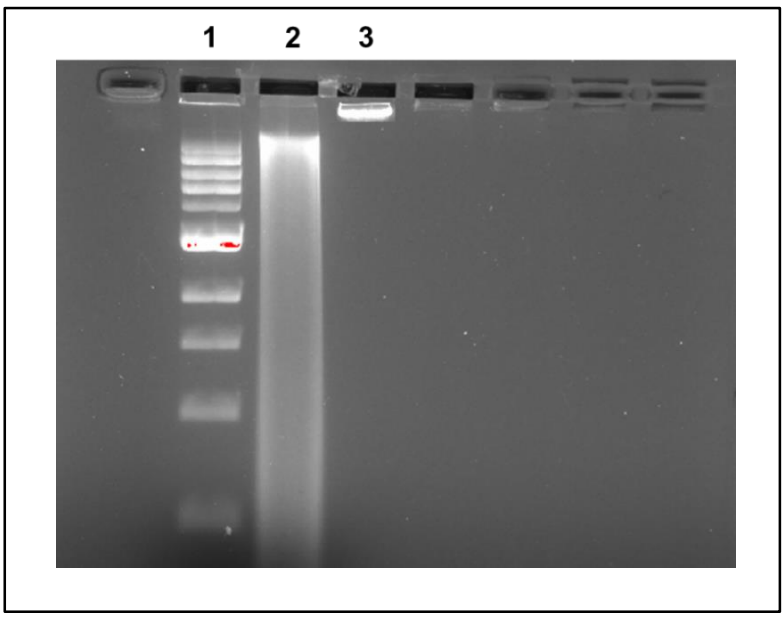

Figure 6.11 Agarose gel electrophoresis analysis of TRPA1 siRNA loading in liposomal: lane 1, DNA ladder marker (50 bp); lane 2, TRPA1 plain siRNA and lane 3, TRPA1 siRNA liposome.

6.5 TRPA1 siRNA based liposomal formulation attenuates chemotherapy-induced mechanical and cold allodynia in rats

TRPA1, a pain-detecting ion channel crucial in the development of Cold-Induced Neuropathic Pain (CINP), was initially identified as a noxious cold-activated ion channel. This channel is expressed in sensory neurons alongside TRPV1 and is activated through both direct means, involving covalent modification by various reactive chemicals, and indirect pathways, mediated by G-protein coupled receptors. TRPA1 plays a pivotal role in vivo, serving as a necessary component for sensing noxious reactive chemicals (Takayama et al., 2019). Previous studies have extensively documented its essential role in detecting acute noxious cold and mechanical stimuli (Shibata and Tang, 2021). This study represents a pioneering investigation into the development and application of a liposomal formulation containing TRPA1 siRNA, administered intravenously for the attenuation of CINP. Distinct control groups were established, encompassing plain siRNA, a blank formulation without TRPA1 siRNA and liposomal loaded TRPA1 siRNA. Furthermore, the study involved the administration of the same formulation through both intrathecal and intravenous routes. A dosage of 50μg/15μL was administered for plain siRNA, 50 μg/15 μL for the blank formulation, and an equivalent dose of the TRPA1-loaded liposomal formulation using both route of administration. The therapeutic efficacy was assessed by evaluating the alleviation of cold and mechanical hypersensitivity in chemotherapy-treated rats. This marks the first instance of exploring the potential of TRPA1 siRNA through a liposomal formulation, highlighting its effectiveness through different administration routes for managing CINP.

Cold allodynia was indicated by a substantial increase in paw withdrawal scores, while mechanical allodynia was characterized by an elevated paw withdrawal threshold in rats subjected to chemotherapy. In the case of cold allodynia, rats exposed to

chemotherapy displayed heightened sensitivity, as reflected by increased paw withdrawal scores (**Figure 6.12)**. This heightened sensitivity is a common manifestation of neuropathic pain induced by chemotherapy.

The findings demonstrated that the liposomal TRPA1 siRNA formulation effectively mitigated cold pain hypersensitivity in the neuropathic rats. Both modes of administration, intrathecal and intravenous, proved to be successful in reducing the observed sensitivity, emphasizing the versatility and potential therapeutic effect of the liposomal formulation. Moving on to mechanical allodynia, the study observed a significant increase in paw withdrawal thresholds in rats undergoing chemotherapy. This heightened mechanical sensitivity is another characteristic feature of neuropathic pain induced by chemotherapy. Recognizing the clinical limitations of the intrathecal route, we sought to enhance the translational potential by formulating a liposomal version for intravenous administration. Our study involved a three-day regimen, administering 50 µg/15 µL per day via a Hamilton syringe with a 25-gauge needle. Remarkably, the administration of plain siRNA through the intrathecal route resulted in pain attenuation up to the 4^{th} day post-injection, starting from the 2^{nd} day. Notably, our liposomal TRPA1 siRNA formulation exhibited a compelling and unprecedented outcome, attenuating both mechanical and cold pain behaviors from the initial day of injection through the 6^{th} day. This sustained effect underscores the encapsulation efficiency of the liposomal carrier, which ensures a control release profile **(Figure 6.13)**. Our findings represent a significant advancement in the field, demonstrating the efficacy of the encapsulated TRPA1 siRNA formulation in alleviating neuropathic pain via both intravenous and intrathecal routes. The sustained release characteristics of the liposomal carrier contribute to the prolonged therapeutic effect, showcasing the potential for clinical translation and improved patient outcomes. This novel approach holds promise for addressing CINP and opens avenues for further exploration in the realm of pain management.

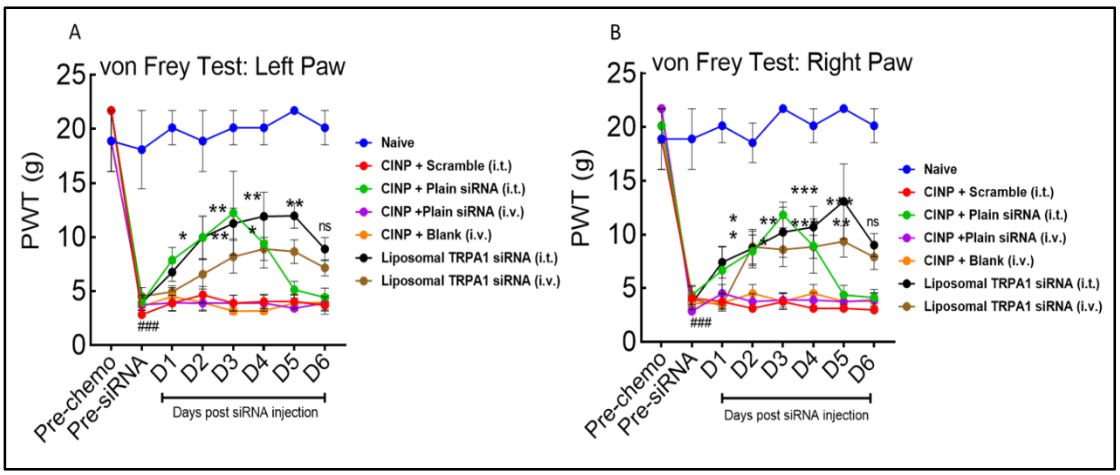

Figure 6.12 Effect of liposomal TRPA1 siRNA formulation on alleviating chemotherapy-induced mechanical allodynia in rats. A substantial elevation in paw withdrawal threshold induced by chemotherapy in rats. TRPA1 siRNA-loaded nanoformulation via intrathecal and intravenous routes effectively mitigated mechanical pain in neuropathic rats. **A)** paw withdrawal threshold in the left paw**. B)** paw withdrawal threshold in the right paw. Results are expressed as mean ± S.E.M. for n = 8-9 rats. Two-way ANOVA followed by Bonferroni's multiple comparison test. ###P<0.001 indicates statistical significance as compared to the naïve rats. *p<0.05, **p<0.01, and ***p<0.001 indicates statistical significance as compared to the pre-siRNA baseline. P<0.05 was considered statistically significant.

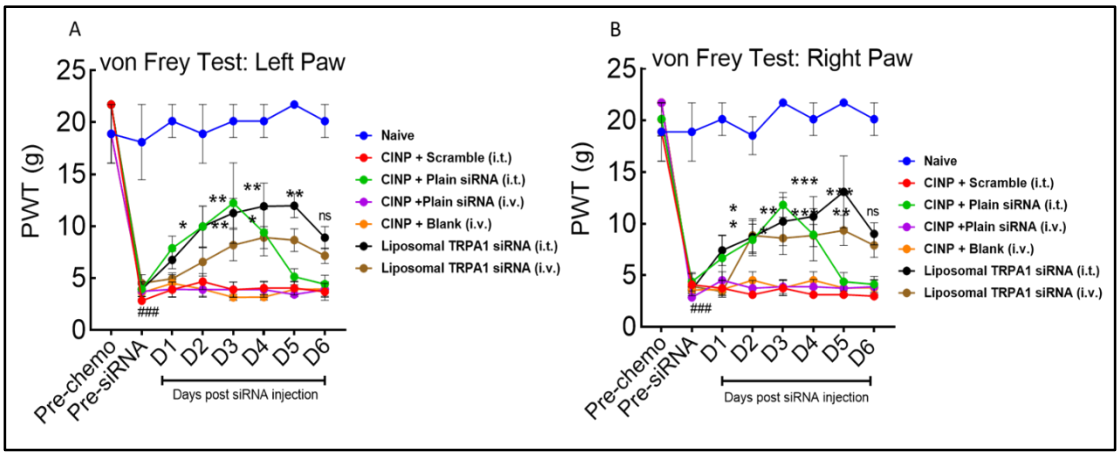

Figure 6.13 Effect of liposomal TRPA1 siRNA formulation on alleviating chemotherapy-induced cold allodynia in rats. A significant increase in paw withdrawal score induced by chemotherapy in rats. administration of TRPA1 siRNA-loaded liposomes via intrathecal and intravenous routes effectively mitigated cold pain hypersensitivity in the neuropathic rats. **A)** paw withdrawal score in the left paw **b)** paw withdrawal score in the right paw. Results are expressed as mean ± S.E.M. for n = 8-9 rats. Two-way ANOVA followed by Bonferroni's multiple comparison test. ###P<0.001 indicates statistical significance as compared to the naïve rats. *p<0.05, **p<0.01, and ***p<0.001 indicates statistical significance as compared to the pre-siRNA baseline. P<0.05 was considered statistically significant.

6.6 TRPA1 siRNA based liposomal formulation downregulates TRPA1 and Iba1 protein expressions in spinal cord of neuropathic rats

Following pain behavioral assessment assays, developed nanoforumulation of TRPA1 siRNA has demonstrated noteworthy efficacy in alleviating CINP through both intrathecal and intravenous administration. Our findings represent the inaugural report proposing the effectiveness of the TRPA1 siRNA formulation administered intravenously in alleviating pain-like behaviors in neuropathic rats. Subsequently, we delved into the molecular intricacies to elucidate the underlying mechanisms. Our investigations revealed that the developed TRPA1 siRNA nanoforumulation significantly reduced spinal TRPA1 ($p<0.001$) and Iba1 ($p<0.001$) protein expressions in rats administered through both intravenous and intrathecal routes, in comparison to their respective control groups. Utilizing one-way ANOVA followed by Tukey's multiple comparison tests, we observed a significant increase in TRPA1 [$F (6, 21) = 69.2$, $P<0.001$] and Iba1[$F (6, 21) = 50.4$, $P<0.001$] protein expressions in the spinal cord of neuropathic rats **(Figure 6.14)**. Treatment with the TRPA1 siRNA liposome formulation, whether administered intravenously and intrathecally, effectively attenuated the heightened protein expressions of both TRPA1 and Iba1 in the lumbar spinal cord of neuropathic rats, showing a substantial reduction compared to the respective control and healthy control groups.

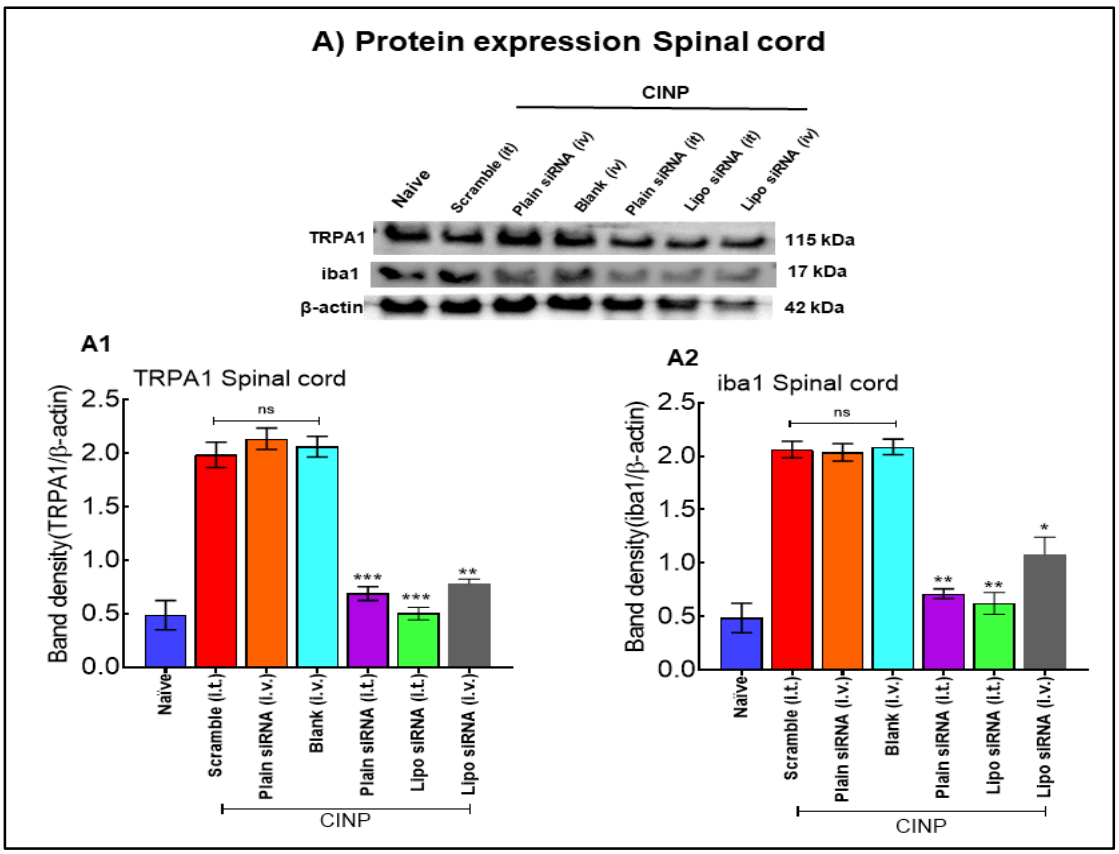

Figure 6.14 Effect of liposomal TRPA1 siRNA formulation on TRPA1 and Iba1 protein expressions in neuropathic rats. TRPA1 siRNA formulation inhibits the TRPA1 mediated Iba1 expressions in spinal cord of neuropathic rats. **A1)** Protein expression of TRPA1 **B1)** Protein expression of Iba1. Data were presented as mean ± SEM. ###P<0.001 indicates statistical significance as compared to healthy rats. *p<0.05, **p<0.01, and ***p<0.001 indicates statistical significance as compared to the vehicle-treated rats. P<0.05 was considered statistically significant. Results are expressed as mean ± S.E.M. n=4.

6.7 Liposomal formulation downregulates ICAM-1 & TNF α protein expressions in spinal cord of neuropathic rats

The activation of TRPA1, a sensory neuron ion channel, appears to exert influence on the expression of ICAM-1 a cell adhesion molecule implicated in inflammatory processes. The interplay between TRPA1 and ICAM-1 in the spinal cord suggests a potential role in mediating neuroinflammation and cellular responses associated with neuropathic conditions. Further comprehension of this molecular relationship could provide valuable insights for targeted therapeutic interventions in

neuropathic pain. Consequently, we investigated the expression of ICAM-1 and TNF-α in neuropathic rats, discovering that our developed liposomal formulation effectively downregulates TRPA1-mediated ICAM-1 and TNF-α protein expressions in the spinal cord **(Figure 6.15).** This downregulation was observed through both intravenous and intrathecal administrations, in contrast to the respective control and healthy naïve groups. Using one-way ANOVA followed by Tukey's multiple comparison tests indicated a significant decrease in ICAM-1 levels [$F(6, 7) = 3.35$, $p<0.001$] and TNF-α [$F(6, 21) = 12.7$, $p<0.001$] respectively in rats administered with TRPA1 siRNA formulation through both intrathecal and intravenous routes compared to their respective control and naïve control groups. These findings suggest a potential therapeutic impact in modulating neuroinflammatory responses associated with neuropathic pain through the developed TRPA1 siRNA liposomal formulation.

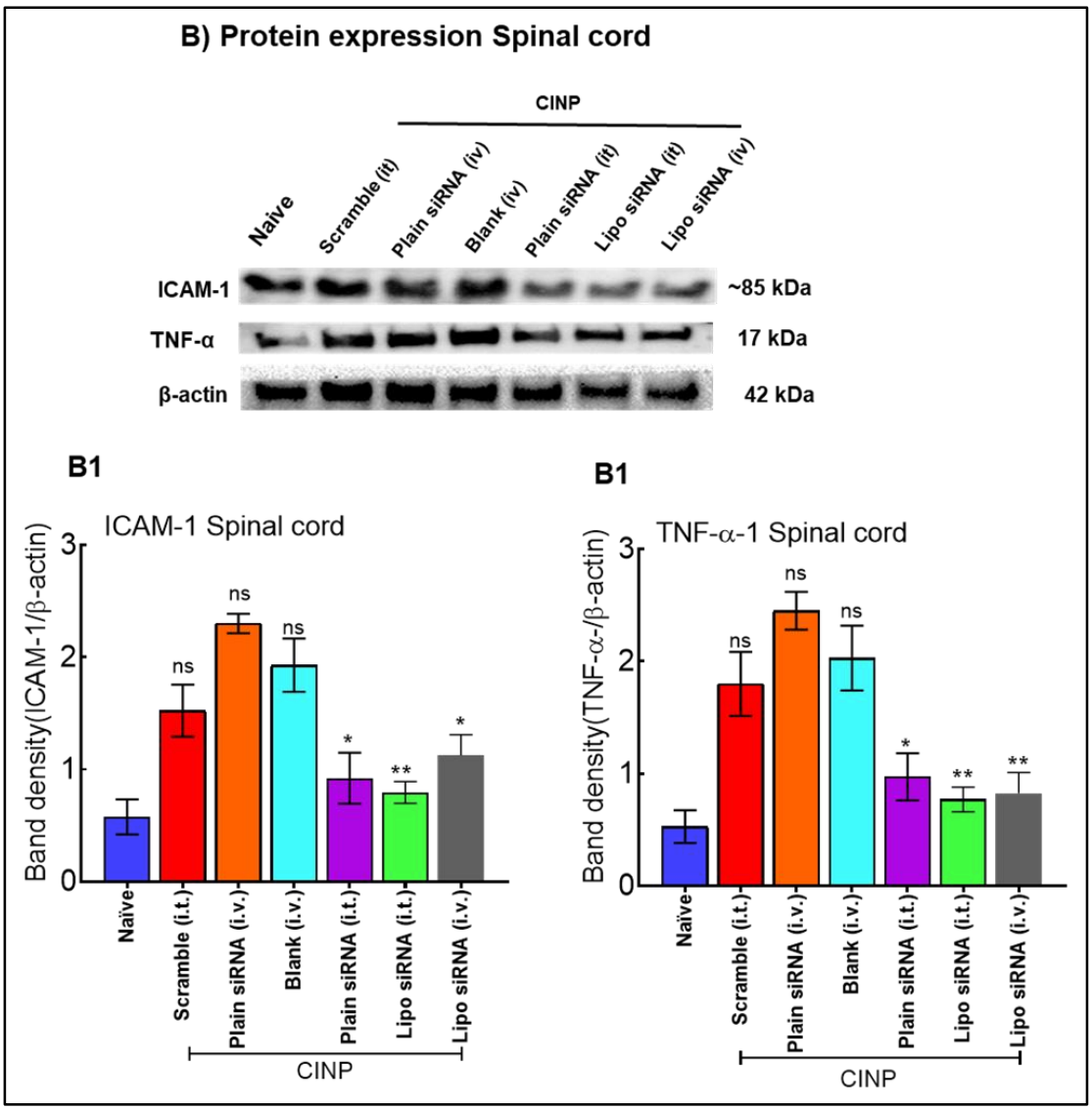

Figure 6.15 Effect of liposomal TRPA1 siRNA formulation on ICAM-1 and TNF-α protein expressions in neuropathic rats. TRPA1 siRNA formulation downregulates the ICAM-1 and TNF-α expressions in spinal cord of neuropathic rats. Data were presented as mean ± SEM. ###P<0.001 indicates statistical significance as compared to healthy rats. *p<0.05, **p<0.01, and ***p<0.001 indicates statistical significance as compared to the vehicle-treated rats. P<0.05 was considered statistically significant. Results are expressed as mean ± S.E.M. n=4.

6.8 Liposomal formulation downregulates TRPA1 and IL-6 mRNA expressions in DRG of neuropathic rats

Our study represents a groundbreaking report, introducing the promising efficacy of intravenously administered TRPA1 siRNA formulation in mitigating pain-

like behaviors in neuropathic rats. Subsequently, we conducted a detailed exploration of molecular intricacies to uncover the underlying mechanisms. Our investigations unveiled that the developed TRPA1 siRNA nanoformulation led to a significant reduction in TRPA1 mRNA ($p<0.05$) and IL-6 expressions in rats, particularly when administered intravenously, as compared to their respective control groups. Employing one-way ANOVA followed by Tukey's multiple comparison tests, we observed a noteworthy decrease in TRPA1 [$F (6, 25) = 69.2$, $P<0.001$] and IL-6 [$F (6, 24) = 50.4$, $P<0.05$] mRNA expressions in the dorsal root ganglia (DRG) of neuropathic rats **(Figure 6.16)**. Interestingly, no significant changes were observed in the mRNA expressions of TRPA1 and IL-6 in the TRPA1 siRNA formulation when administered via the intrathecal route. These findings underscore the specific efficacy of intravenous administration of the TRPA1 siRNA formulation in modulating key molecular targets implicated in neuropathic pain, opening new avenues for targeted therapeutic interventions.

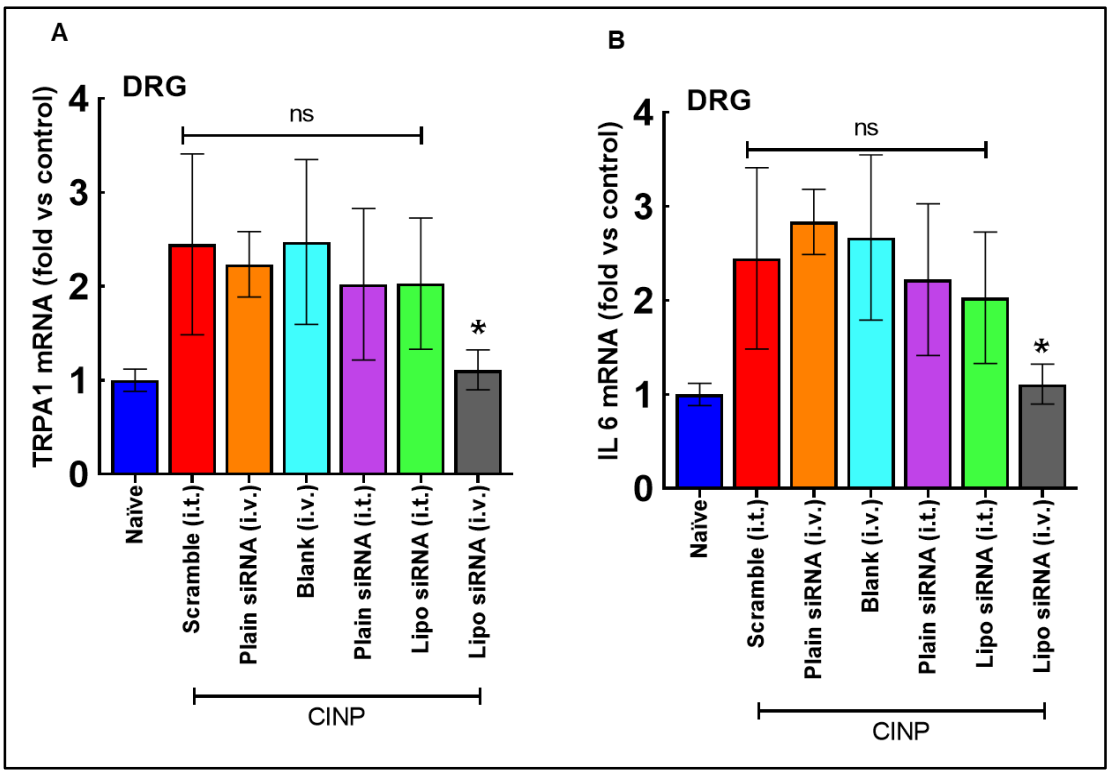

Figure 6.16 Effect of liposomal TRPA1 siRNA formulation on TRPA1 and IL6 mRNA expressions in neuropathic rats. TRPA1 siRNA formulation downregulates the TRPA1 and IL-6 expressions in DRG of neuropathic rats. Data were presented as mean ± SEM. ###P<0.05 indicates statistical significance as compared to healthy rats. *p<0.05, indicates statistical significance as compared to the vehicle-treated rats. P<0.05 was considered statistically significant. Results are expressed as mean ± S.E.M. n=4.

6.9 TRPA1 siRNA formulations does not affect locomotor activity and motor coordination of rats

The effect of the TRPA1 siRNA formulation on the locomotor activity and motor coordination of rats was comprehensively assessed through open field and rota-rod tests. These evaluations were conducted following both intrathecal and intravenous administration routes to ensure a thorough understanding of any potential central side effects. In the open field test, rats treated with plain siRNA and TRPA1-based siRNA liposomal formulations via both intrathecal and intravenous routes exhibited no discernible differences in average speed and total distance traveled. The absence of significant disparities in total traveled distance and average speed implies that the

developed formulation does not induce any locomotor impairment in the animals **(Figure 6.17 A-D).** Furthermore, the Rota rod test revealed that the TRPA1 siRNA formulation, regardless of whether administered intravenously or intrathecally, did not result in any significant differences in the time spent on the rotarod compared to the pre-drug baselines **(Figure 6.17 E)**. This observation further supports the conclusion that the developed TRPA1 siRNA formulation does not adversely affect motor coordination in rats. In summary, our comprehensive behavioral assessments using open field and rota-rod tests provide robust evidence that the developed TRPA1 siRNA liposomal formulation, administered through both intrathecal and intravenous routes, does not elicit any detrimental effects on the locomotor activity or motor coordination of rats. These findings enhance the safety profile of the formulation, positioning it favorably for further exploration as a potential therapeutic intervention.

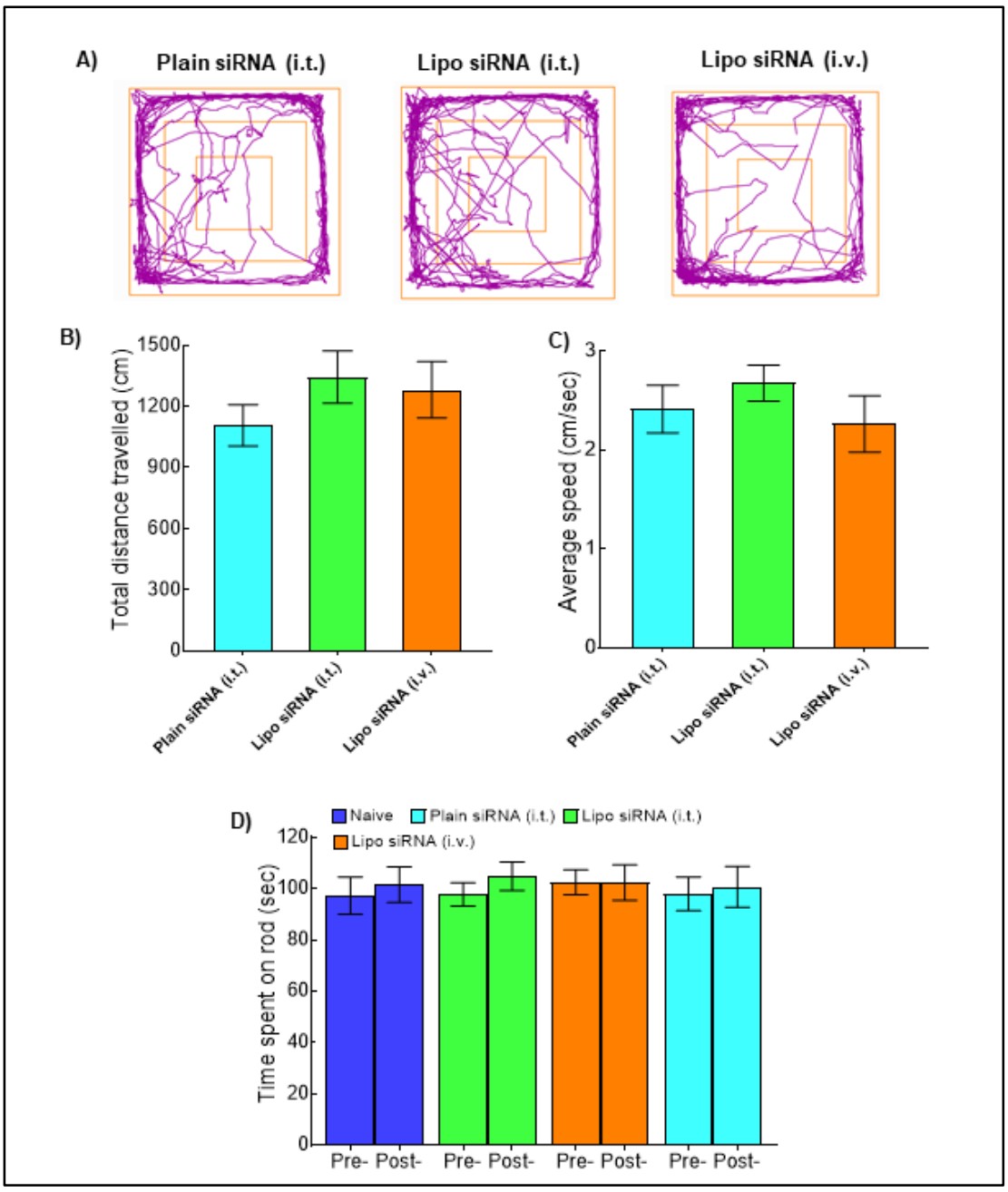

Figure 6.17 Effect of the TRPA1 siRNA-based nano-formulation on the locomotor activity and motor coordination of rats with CINP. Open Field Test: (A) Open field track plots depicting the movement patterns of CINP rats treated with plain siRNA (intrathecal, i.t.), Lipo siRNA (intrathecal, i.t.), and Lipo siRNA (intravenous, i.v.) were examined. **(B)** The total distance traveled in the open field arena and **(C)** the average speed of rats in each treatment group were quantified. Remarkably, the treatment with TRPA1 siRNA-based nanofomulation did not induce any significant alterations in the locomotor activity of neuropathic rats, as evidenced by comparable total distance traveled and average speed, when compared to their respective control groups. Statistical analysis using one-way ANOVA followed by Tukey's post hoc analysis

confirmed the lack of significant differences (n=6-7, ***p<0.001, indicating statistical significance compared to the vehicle-treated rats). **Rotarod Test: (D)** In the rotarod test, the time spent by rats on the rotating rod after TRPA1 siRNA formulation treatment was compared to their pre-siRNA baseline. The results demonstrated that the TRPA1 siRNA formulation did not alter the time spent on the rotarod, indicating that it did not adversely affect the motor coordination of the rats. Statistical analysis conducted using two-way ANOVA (Bonferroni's multiple comparison) supported these findings (n=6, **p<0.01, and ***p<0.001, indicating statistical significance compared to the pre-drug baseline). A significance level of $p<0.05$ was considered for all statistical analyses.

In summary, our rigorous behavioral assessments using open field and rotarod tests provide compelling evidence that the TRPA1 siRNA-based nanoforumulation, administered via intrathecal and intravenous routes, does not disrupt the locomotor activity or motor coordination of rats with chronic inflammatory neuropathic pain, enhancing its safety profile for potential therapeutic applications.